Antimicrobial and Healing Efficacy of Sustained Release Nitric Oxide Nanoparticles Against *Staphylococcus Aureus* Skin Infection

Luis R. Martinez[1,2,6], George Han[3,6], Manju Chacko[3], Mircea Radu Mihu[1,2], Marc Jacobson[4,5], Phil Gialanella[4], Adam J. Friedman[3,5,7], Joshua D. Nosanchuk[1,2,7] and Joel M. Friedman[3,7]

Staphylococcus aureus (*SA*) is a leading cause of both superficial and invasive infections in community and hospital settings, frequently resulting in chronic refractory disease. It is imperative that innovative therapeutics to which the bacteria are unlikely to evolve resistance be developed to curtail associated morbidity and mortality and ultimately improve our capacity to treat these infections. In this study, a previously unreported nitric oxide (NO)-releasing nanoparticle technology is applied to the treatment of methicillin-resistant *SA* (MR*SA*) wound infections. The results show that the nanoparticles exert antimicrobial activity against MR*SA* in a murine wound model. Acceleration of infected wound closure in NO-treated groups was clinically shown compared with controls. The histology of wounds revealed that NO nanoparticle treatment decreased suppurative inflammation, minimal bacterial burden, and less collagen degradation, providing potential mechanisms for biological activity. Together, these data suggest that these NO-releasing nanoparticles have the potential to serve as a novel class of topically applied antimicrobials for the treatment of cutaneous infections and wounds.

Journal of Investigative Dermatology (2009) **129,** 2463–2469; doi:10.1038/jid.2009.95; published online 23 April 2009

INTRODUCTION

Staphylococcus aureus (*SA*) is an immotile Gram-positive coccus that frequently colonizes human nasal membranes and skin. This bacterium is responsible for the majority of superficial and invasive skin infections, resulting in more than 11,000,000 outpatient/emergency room visits and 464,000 hospital admissions annually in the United States (Daum, 2007). Furthermore, certain *SA* clinical strains have recently evolved resistance to vancomycin, an antibiotic to which staphylococci have been uniformly sensitive. Although the vancomycin-resistant strains remain rare, methicillin-resistant strains (methicillin-resistant *SA*, MR*SA*) are increasingly common (Hiramatsu *et al.*, 1997), highlighting the urgent need to develop new approaches for the treatment of *SA* infections.

Topically applied nitric oxide (NO) is a potentially useful preventive and therapeutic strategy against superficial skin infections, including MR*SA* infections (Ghaffari *et al.*, 2006). NO modulates immune responses (Mowbray *et al.*, 2009) and is a significant regulator of wound healing (Soneja *et al.*, 2005). We have recently developed an inexpensive, stable, and rapidly deployable NO-releasing platform using silane hydrogel-based nanotechnology (Friedman *et al.*, 2008). The sustained release rate and total concentration of NO can be modulated by altering the methods for nanoparticle production, for example, by changing the molecular weight of polyethylene glycol or the concentration of nitrite encapsulated. Moreover, our platform benefits from the presence of chitosan, which has been shown to have a potent antimicrobial activity against bacteria (Rabea *et al.*, 2003; Qi *et al.*, 2004). This natural polymer derived from crustacean exoskeletons binds to and disrupts the cell wall and the membrane of microorganisms because of its cationic charge in weakly acidic environments.

In this study, we investigate the applicability of topically applied NO through nanoparticles (NO-np) to *SA* skin infections. On the basis of our earlier work (Friedman *et al.*, 2008), we hypothesized that NO-np can be microbicidal to bacteria in an *in vivo* setting. To validate this hypothesis, we

[1]*Division of Infectious Diseases, Departments of Medicine, Albert Einstein College of Medicine, Bronx, New York, USA;* [2]*Department of Microbiology and Immunology, Albert Einstein College of Medicine, Bronx, New York, USA;* [3]*Department of Physiology and Biophysics, Albert Einstein College of Medicine, Bronx, New York, USA;* [4]*Department of Pathology, Montefiore Medical Center, Bronx, New York, USA and* [5]*Division of Dermatology, Department of Medicine, Montefiore Medical Center, Bronx, New York, USA*

[6]*All these authors contributed equally to this work.*

[7]*These authors share senior authorship.*

Correspondence: Dr Joshua D. Nosanchuk, Department of Medicine, Albert Einstein College of Medicine, 1300 Morris Park Avenue, Bronx, New York 10461, USA. E-mail: nosanchu@aecom.yu.edu

Abbreviations: CFU, colony forming unit; MRSA, methicillin-resistant Staphylococcus aureus*; MSSA, methicillin-sensitive* Staphylococcus *aureus; NO, nitric oxide; NO-np, nitric oxide through nanoparticle; PBS, phosphate-buffered saline*

Received 3 November 2008; revised 26 January 2009; accepted 6 March 2009; published online 23 April 2009

investigated the biological effect of NO-np on *SA* using a mouse infection model.

RESULTS

Detection of NO-np release using amperometric analysis

Amperometric analysis revealed immediate NO release after the addition of NO-np to the solution (Figure 1). The observed trace indicates a relatively stable rate of NO release with only a slight initial peak at 70 minutes. A steady-state level was achieved after 6 hours, maintained for 9 hours, and ongoing release occurred for ~24 hours (data not shown). Transmission electron microscopy reveals that the individual NO-nps are ~10 nm in diameter (Figure 1; inset).

Staphylococcus aureus is susceptible to NO-np

We determined the susceptibility of clinical MR*SA* and MS*SA* (methicillin-sensitive *SA*) strains to NO-np. The minimum inhibitory concentration range for NO-np against 11 MR*SA* strains was 312–2,500 μg ml^{-1} (corresponding to 4.69 nM NO for the initial peak; 3.125 nM for steady state to 37.5 nM for the initial peak; 25 nM for steady state), whereas the range for NO-np for 9 MS*SA* strains was 312–1,250 μg ml^{-1} (4.69 nM NO for the initial peak; 3.125 nM for steady state to 18.75 nM for the initial peak; 12.5 nM for steady state) (Table 1).

SA damage caused by NO-np was monitored by transmission electron microscopy (Figure 2). Unexposed bacteria showed uniform density in cytoplasmic compartments and cell separation by a cross-wall surrounding a highly contrasting splitting system (Figure 2a). After NO-np treatment, the cross-wall began to disappear (1 hour after treatment; Figure 2b) and cellular edema was visible (4 hours; Figure 2c), followed by the destruction of cell wall architecture (7 hours; Figure 2d) and subsequent cell lysis (24 hours; Figure 2e).

NO increased wound-healing rate in mice

The effect of NO-np on wound healing in Balb/c mice was investigated (Figure 3a and b). Application of NO-np ectopically onto wounds decreased the size of eschar significantly (Figure 3b). At day 3, the size of eschar of uninfected or MR*SA*-infected wounds treated with NO-np reached ~2.75 mm, whereas the size of eschar of untreated or nanoparticles only (np particles containing the same formulation as NO-np, but without NO precursor or release) treated wounds was ~4 mm for the uninfected groups ($P<0.05$) and ~5.5 mm in the MR*SA*-infected untreated or np-treated groups ($P<0.001$; as compared with NO-np treated groups). At day 7 (Figure 3b), the size

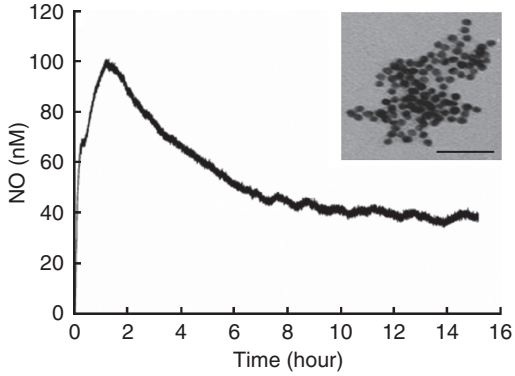

Figure 1. Amperometric real-time detection of NO-np released. Kinetics of nitric oxide (NO) release in solution was measured using amperometric analysis. The inset TEM photograph shows uniform nitric oxide through nanoparticles (NO-np) of ~10 nm in diameter. Bar = 100 nm.

Table 1. Susceptibility of *Staphylococcus aureus* to commonly used antimicrobial drugs and nitric oxide

Organism and antimicrobial agent	*n*	Range (μg ml^{-1})	% S[1]
S. aureus MRSA	11		
Ciprofloxacin		⩽0.5–⩾8	27.3
Clindamycin		⩽0.25–⩾8	54.6
Erythromycin		⩽0.25–⩾8	18.2
Gentamicin		⩽0.5–8	72.8
Oxacillin		⩾4	0
Penicillin-G		⩾0.5	0
Rifampin		⩽0.5–1	0
Tetracycline		⩽1–⩾16	90.9
Trimethoprim/Sulfa		⩽10–⩾320	90.9
Vancomycin		⩽1–2	100
Levofloxacin		⩽0.125–⩾8	27.3
Quinupristin/Dalfopr		⩽0.25-0.5	100
Nitrofurantoin		⩽16–32	100
Linezolid		1–2	100
Moxicloxacin		⩽0.25–⩾8	63.6
Nitric Oxide		312–2500[2]	100
S. aureus MSSA	9		
Ciprofloxacin		⩽0.5–⩾8	88.9
Clindamycin		⩽0.25	100
Erythromycin		⩽0.25-0.5	100
Gentamicin		⩽0.5	100
Oxacillin		⩽0.25-0.5	100
Penicillin-G		0.125–⩾0.5	0
Rifampin		⩽0.5	100
Tetracycline		⩽1–⩾16	88.9
Trimethoprim/Sulfa		⩽10	100
Vancomycin		⩽1	100
Levofloxacin		⩽0.125–⩾8	88.9
Quinupristin/Dalfopr		⩽0.25-0.5	100
Nitrofurantoin		⩽16–64	100
Linezolid		2	100
Moxicloxacin		⩽0.25–2	100
Nitric oxide		312–1250[2]	100

MR*SA*, methicillin-resistant *Staphylococcus aureus*; MS*SA*, methicillin-sensitive *Staphylococcus aureus*.
[1]Percentage of isolates susceptible based on Clinical and Laboratory Standards Institute guidelines.
[2]5,000 μg ml^{-1} is equal to 75 nM in solution for initial peak; 50 nM in solution for steady state.

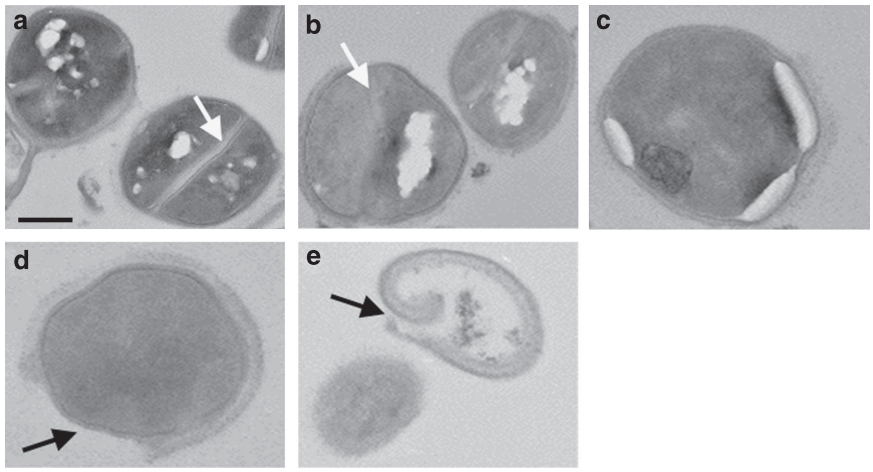

Figure 2. NO-releasing nanoparticles have antimicrobial activity against *SA*. TEM of *SA* exposed to sustained release of NO by nanoparticles revealed cell wall damage and lysis. (**a**) Growth of *SA* in the absence of NO-np showed intact cell wall architecture (control). Growth of *SA* in the presence NO-np after 1 (**b**), 4 (**c**), 7 (**d**), and 24 hours (**e**) showed increasing destruction of cell wall architecture, edema, and cell lysis. White and black arrows denote bacterial cross-wall and cell wall damage after NO treatment, respectively. Bar = 0.2 μm.

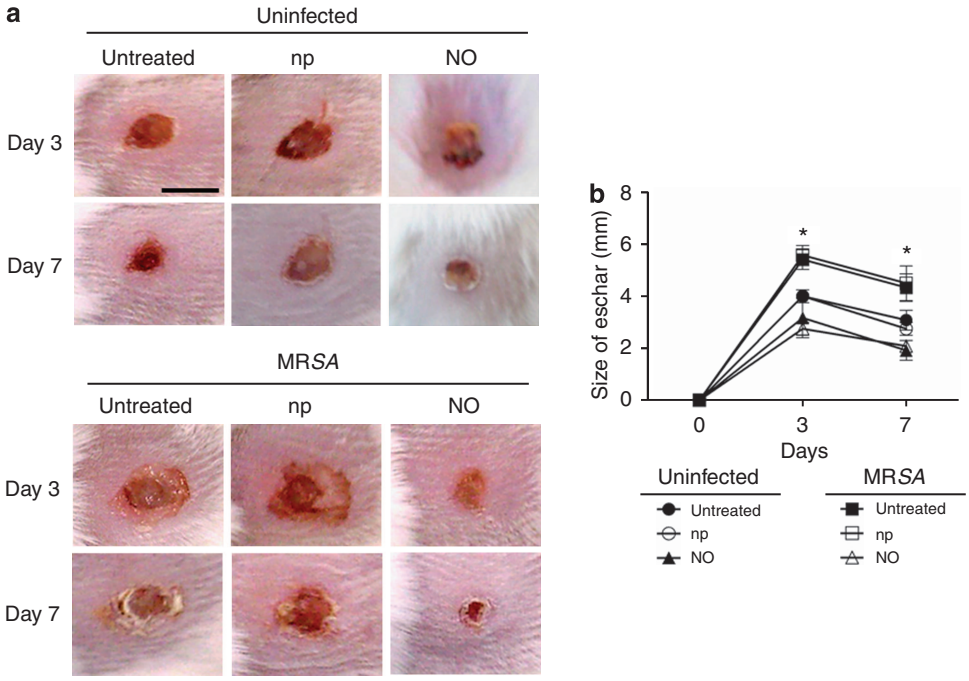

Figure 3. NO-np increased the wound healing rate in mice. (**a**) Wounds of Balb/c mice uninfected and untreated, uninfected treated with nanoparticles without nitric oxide (NO) (np), uninfected treated with nitric oxide through nanoparticle (NO-np,) untreated methicillin-resistant *Staphylococcus aureus* (MR*SA*)-infected, np-treated MR*SA*-infected, and MR*SA*-infected treated with NO-np, days 3 and 7. Bar = 5 mm. (**b**) Wound size analysis of Balb/c mice skin lesions. Wounds were uninfected or infected with MR*SA* and untreated or treated in the absence or presence of NO. Time points are the averages of the results for ten measurements, and error bars denote SDs. **P* < 0.05 in comparing the NO-treated groups with uninfected or MR*SA*-infected and untreated groups.

of eschar of the wounds of groups treated with NO-np was ~2 mm, whereas the size of eschar of untreated or np-treated wounds reached ~3 mm for the uninfected groups ($P<0.05$) and ~4.5 mm for the MR*SA*-infected untreated or np-treated groups ($P<0.01$).

NO killed MR*SA* in superficial skin lesions

The efficacy of NO-np in killing *SA* in mice was further explored by examining the bacterial burden in these skin infections. Four days after infection, wounds were swabbed and plated on tryptic soy agar. MR*SA*-infected NO-np-treated wounds showed significantly lower microbial burden than did the untreated or np-treated wounds ($P<0.01$) (Figure 4a). Furthermore, to confirm percutaneous bacterial penetration of the epidermal tissue and to show the efficacy of NO in controlling bacterial infection, the infected skin tissue was removed from mice that were killed at day 7 after infection and the bacterial burden determined. MR*SA*-infected

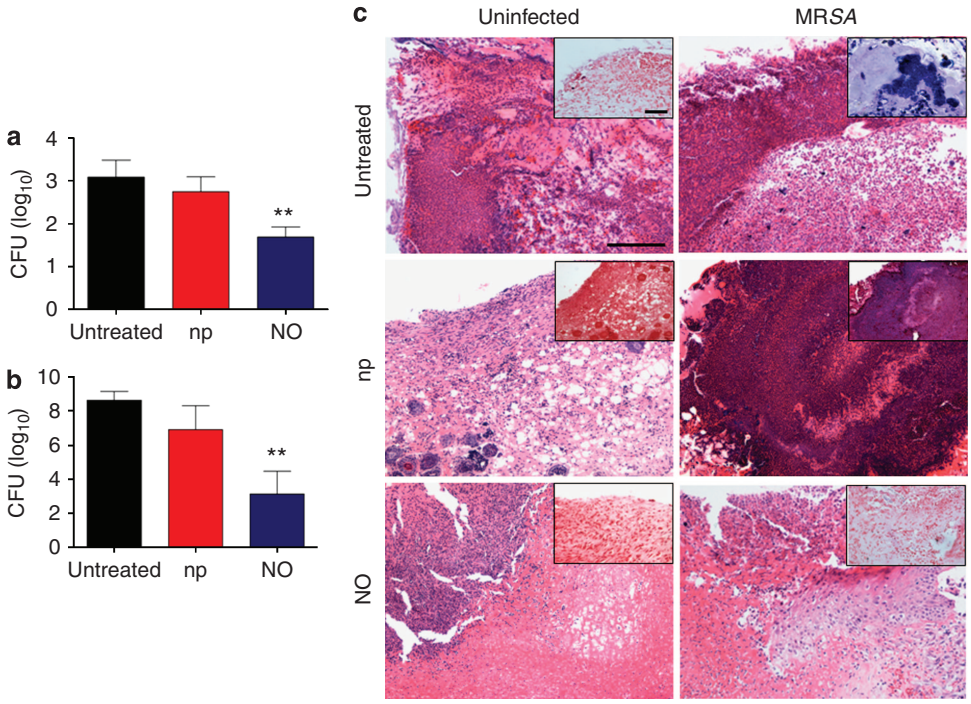

Figure 4. NO-np killed MR*SA* in superficial skin lesions. (**a**) Wound bacterial burden (CFU; colony forming unit) in NO-treated mice infected intradermally with 10^7 methicillin-resistant *Staphylococcus aureus* is significantly lower than untreated or NP-treated mice ($n=10$ per group). Four days after infection, wounds were swabbed and bacteria burden examined. (**b**) Seven days after infection, infected skin tissue was removed from mice and bacterial burden determined. Uninfected mice untreated, NP-, and NO-treated were used as a control. Bars are the averages of the results for three measurements, and error bars denote standard daviations. Asterisks denote *P*-value significance (**$P<0.01$) calculated by analysis of variance and adjusted by use of the Bonferroni correction. (**c**) Histological analysis of BALB/C mice uninfected and untreated, uninfected treated with nanoparticles without NO (NP), uninfected treated with NO-NP (NO), untreated MR*SA*-infected, NP-treated MR*SA*-infected, and MR*SA*-infected treated with NO, day 7. Mice were infected with 10^7 MR*SA* bacterial cells. Representative H&E-stained sections of the skin lesions are shown with the *insets* representing Gram staining specific for MR*SA* cells (shown in purple). Scale bars = 25 μm.

mice treated with NO-np had significantly lower microbial burden than did the untreated or np-treated mice ($P<0.01$) (Figure 4b). In both assays, <30 colony forming units (CFUs) were detected in the skin of uninfected mice and *SA* was not identified.

Histological examinations revealed that wounds of untreated or np-treated uninfected mice had intense inflammatory infiltrate in the absence of bacteria by Gram stains (Figure 4c). Analysis of MR*SA*-infected wounds, both untreated and np-treated, showed an even more severe neutrophil-rich infiltrate along with extensive cell necrosis. Tissue Gram stains of these samples revealed large numbers of Gram-positive cocci (Figure 4c; insets). Tissue sections from the wounds of NO-np-treated uninfected mice and MR*SA*-infected mice revealed less suppurative inflammation along with increased fibrin deposition and no evidence of bacteria (Figure 4c).

NO-np enhances wound healing by preventing MR*SA* collagen degradation

The mechanisms through which the NO-nps accelerate wound healing were further determined by establishing whether NO-nps prevented collagen degradation by MR*SA* in the infected tissue. Collagen content was highest in both uninfected and infected wounds treated with NO-nps, although np-treated uninfected tissue also had high collagen content (Figure 5a). The dispersed blue stain indicated thicker and more mature tissue collagen formation in wounds treated with NO-np, suggesting that NO-np exposure maintained dermal architecture through bacterial clearance, and ultimately by guarding collagen. Figure 5b is a morphometric analysis of the data shown in Figure 5a.

DISCUSSION

Many investigations have suggested the important role of NO in immunity and the wound-healing process, and therefore the potential applications are broad and the implications multidisciplinary. With respect to this study, the nanoparticulate powder could be used in the treatment of numerous types of wounds, such as burns and decubiti. Furthermore, wound healing complicated by common comorbidities, such as obesity, diabetes, atopic dermatitis, and peripheral vascular disease may benefit from an NO-based therapeutic. Specifically, diabetics are prone to chronic leg and foot ulcerations caused by abnormalities in NO production resulting in both neurological and vascular complications (Honing *et al.*, 1998). The avascular nature of these wounds and the colonization/infection of resistant bacterial species have undermined the efficacy of conventional treatments and

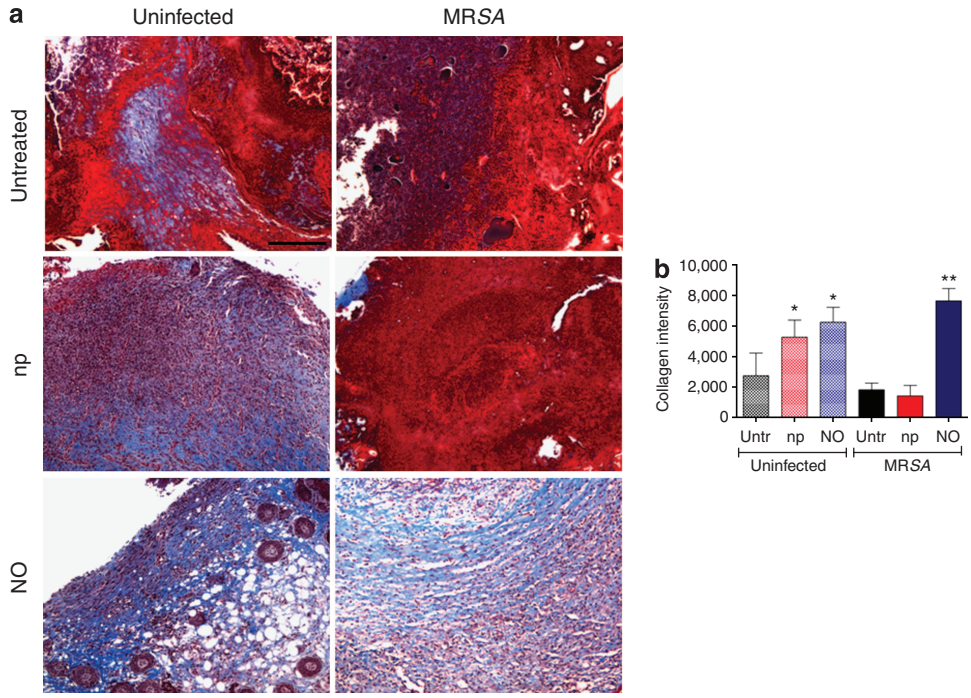

Figure 5. NO-nps decrease collagen degradation in skin lesions of Balb/c mice. (**a**) Histological analysis of Balb/c mice uninfected and untreated (Untr), uninfected treated with nanoparticles without nitric oxide (NO) (np), uninfected treated with NO-nps (NO), untreated methicillin-resistant *Staphylococcus aureus* (MR*SA*)-infected, np-treated MR*SA*-infected, and MR*SA*-infected treated with NO, day 7. Mice were infected with 10^7 bacterial cells. The blue stain indicates collagen. Bar = 25 μm. (**b**) Quantitative measurement of collagen intensity in 16 representative fields of the same size for uninfected and untreated, uninfected treated with nanoparticles without NO (np), uninfected treated with NO, untreated MR*SA*-infected, np-treated MR*SA*-infected, and MR*SA*-infected treated with NO wounds. Bars are the averages of the results, and error bars denote SDs. *$P<0.01$ in comparing the untreated groups with the uninfected np- and NO-treated groups; **$P<0.001$ in comparing the untreated groups with the MR*SA* + NO group.

also underscored the need for a previously unreported therapeutic approach, such as the sustained delivery of NO, as addressed in this study.

We showed that the beneficial effect of the NO-np treatment on wound closure is likely because of antimicrobial activity and the promotion of collagen deposition. In wound healing, collagen synthesis can be correlated with fibroblast proliferation and differentiation (Schaffer *et al.*, 1996). However, with regard to these findings, it is possible that pre-existing collagen in the wound bed may have limited the precision of our analysis. Therefore, we are pursuing further in-depth investigations of these observations through specific markers of re-epithelization, such as pro-collagen and elastin, and markers of angiogenesis, such as CD31.

With regard to this specific NO delivery platform, the stability of the compound combined with the simplicity of treatment makes NO-nps ideal for combat or disaster situations; soldiers or emergency personnel could carry packets with NO-np and topically apply it to traumatic wounds in the field to combat microbial infections before receiving expert medical care. Topically applied NO has been effective in inducing a local immune response with minimal inflammation (Mowbray *et al.*, 2009), further adding to its beneficial effects in this application.

With regard to safety and toxicity, the cytotoxic potential for nanotechnologies has been well documented and widely commented on (Service 2003; Nel *et al.*, 2006). Numerous investigations have revealed that diverse nanomaterials can penetrate intact skin in animal models and in human *ex vivo* models (Chang *et al.*, 2006; Gamer *et al.*, 2006; Baroli *et al.*, 2007). Furthermore, cutaneous penetration can be enhanced depending on the delivery vehicle or barrier disruption, especially in cases of open wounds, such as those that we describe in this study. Of greater concern, toxicities caused by the systemic penetration and ultimate circulation of specific nanomaterials through various orifices have been shown (Afaq *et al.*, 1998; Hohr *et al.*, 2002). We have shown *in vitro* that NO-nps show minimal toxicity toward cultured fibroblasts (Friedman *et al.*, 2008). Furthermore, *in vivo* safety (murine) evaluation through intraperitoneal and intravenous administration revealed minimal serologically determined cytotoxicity and no clinical adverse events (Cabrales P, personal communication).

In summary, the presented data show that NO-nps have both antimicrobial and wound-healing properties. Overall, the presented results show that the topical application of NO-nps is highly effective against cutaneous MR*SA* infection in a murine model. In addition, the NO-nps appear to enhance wound healing by shielding dermal structural components, such as collagen from degradation. These results suggest that this platform has the potential to serve as a previously unreported, to our knowledge, easily administered class of topical antimicrobials for the treatment of cutaneous infections and wounds.

MATERIALS AND METHODS

SA clinical isolates

The *SA* clinical isolates used in this study were collected from patients' wounds at the Montefiore Medical Center, Bronx, NY. All samples were obtained with the written consent of all patients according to the practices and standards of the institutional review boards at the Albert Einstein College of Medicine and Montefiore Medical Center. In addition, all studies were conducted according to the Declaration of Helsinki Principles. A total of 20 clinical isolates were studied, including 11 MR*SA* and 9 MS*SA* strains, which were stored in a BHI broth (BBL, Cockeysville, MD) containing 40% glycerol at −80 °C until use, and then were grown in a Tryptic Soy broth (TSB; MP Biomedicals, LLC, Solon, OH) overnight at 37 °C with rotary shaking at 150 r.p.m. Their growth was monitored by measuring the optical density at 600 nm (Bio-Tek, Winooski, VT).

Synthesis of NO-np

The synthesis of NO-np was recently reported along with its potential as a treatment for superficial infections (Friedman *et al.*, 2008). Briefly, a hydrogel/glass composite was synthesized using a mixture of tetramethylorthosilicate, polyethylene glycol, chitosan, glucose, and sodium nitrite in a 0.5 M sodium phosphate buffer (pH 7). The nitrite was reduced to NO within the matrix because of the glass properties of the composite effecting redox reactions initiated with thermally generated electrons from glucose. After redox reaction, the ingredients were combined and dried using a lyophilizer, resulting in a fine powder comprising nanoparticles containing NO. Once exposed to an aqueous environment, the hydrogel properties of the composite allow for an opening of the water channels inside the particles, facilitating the release of the trapped NO over extended time periods.

Amperometric detection of NO release

Amperometric detection of NO released from the nanoparticles was achieved using the Apollo 4000 Nitric Oxide Detector (World Precision Instruments, Sarasota, FL). The system is based on a composite graphite NO-sensing element coated with an NO-selective membrane coupled with a reference electrode and can sense NO levels down to the subnanomolar range (Zhang and Broderick, 2000). Out of numerous sensor tips, the ISO-NOP sensor (World Precision Instruments Ltd., Sarasota, FL) was used because of its detection limits (1 nM minimum), quick response time, and specificity toward NO. Briefly, argon degassed 0.05 M phosphate buffer was saturated with NO gas, resulting in a 1.9 mM solution of NO. The probe on the NO detector system was allowed to equilibrate with 20 ml of 0.05 M phosphate buffer under stirring. Aliquots of the saturated NO solution were added and the resulting data were used to construct a linear calibration curve. Data were generated by allowing the system to equilibrate with 20 ml of 0.05 M phosphate buffer under stirring and then adding 100 mg of NO-np. Data were then collected over time and correlated with the calibration data, resulting in measurements of NO concentration in solution over time.

Susceptibility of MR*SA* and MS*SA* strains to NO-np

To evaluate the susceptibility of *SA* to NO-np, a suspension of 10^7 *SA* cells were incubated in an Eppendorf tube with 1 ml of DMEM (Mediatech, Herndon, VA) containing NO-np (0.313, 0.625, 1.25, 2.5, or 5 mg ml^{-1}). A tube containing bacteria with DMEM alone was used as a control. Bacteria and nanoparticles were constantly mixed using a tube rotator (ATR, Laurel, MD) to ensure uniform distribution and incubated at 37 °C for 2 hours. CFU counts were assessed to determine the toxicity of NO on bacterial mass. After incubation with NO-np, a volume of 100 µl of suspension containing bacteria was aspirated and transferred into another Eppendorf tube with 900 µl of phosphate-buffered saline (PBS), and vortexed gently. The suspensions were serially diluted in PBS and aliquots were plated on tryptic soy agar plates. The percentage of CFU survival was determined by comparing the survival of NO-treated *SA* cells relative to the survival of untreated bacteria.

NO treatment and skin infection

Skin and soft tissue are the most common sites of *SA* infection and comprise more than 75% of MR*SA* disease. To simulate this pattern of *SA* exposure, the hair on the back of female Balb/c mice (6–8 weeks; National Cancer Institute, Frederick, MD) was shaved and the skin disinfected with ethanol. Single punch biopsies were performed on the back of the mice, resulting in 5-mm diameter full-thickness excision wounds. Thereafter, a suspension containing 10^7 *SA* 6498 in PBS was inoculated directly onto the wound and 5 mg of the lyophilized NO-np or np powder was topically applied 1 and 72 hours after biopsy. *SA* 6498 is a clinical isolate that was selected for this experiment, because the strain is resistant to diverse commonly used antibiotics. Untreated mice were used as an additional control. Photographs of the wounds were taken daily to follow gross visual wound healing as assessed by the area of the wound uncovered by the migrating epithelia. On day 7 after biopsy, mice were killed and histological sections of the wound area were obtained for analysis.

Histological processing of skin infection model

On day 7 after MR*SA* inoculation, skin lesion tissues were excised from mice that were killed, fixed in 10% formalin for 24 hours, processed, and embedded in paraffin. Four-micron vertical sections were fixed to glass slides, hematoxylin and eosin, Gram, or Masson's trichrome stained to observe the morphology, bacteria, or collagen deposition, respectively, and examined using light microscopy.

The CFU determinations are:

(i) **Superficial examination.** At day 4 after MR*SA* inoculation, a wet swab with sterile PBS was applied superficially to the wounds of the mice and plated on tryptic soy agar.

(ii) **Wound examination.** At day 7 after MR*SA* inoculation, skin lesion tissues were homogenized in sterile PBS and plated on tryptic soy agar.

Eschar size analysis using a mouse skin infection model

Ten mice in each group were examined. Wound size analysis was performed on days 3 and 7 after initial surgery. Histological sections were prepared, and the maximal diameter of each eschar was measured using light microscopy.

Transmission electron microscopy

Transmission electron microscopy was used to visualize NO-np and *SA*. Samples were fixed in 2.5% glutaraldehyde in 0.1 M cacodylate

buffer at room temperature for 2 hours and then incubated overnight in 4% formaldehyde, 1% glutaraldehyde, and 0.1% PBS. The samples were incubated for 90 minutes in 2% osmium tetroxide, serially dehydrated in ethanol, and embedded in Spurr's epoxy resin. Thin sections were obtained on a Reichert Ultracut (Austria) and stained with 0.5% uranyl acetate and 0.5% lead citrate. Samples were observed in a JEOL 1200EX transmission electron microscope (JEOL Ltd., Tokyo, Japan) operating at 80 kV.

Statistical analysis

All data were subjected to statistical analysis using GraphPad Prism 5.0 (GraphPad Software, La Jolla, CA). *P*-values were calculated by analysis of variance and were adjusted by use of the Bonferroni correction. *P*-values of <0.05 were considered significant.

CONFLICT OF INTEREST

The authors state no conflict of interest.

ACKNOWLEDGMENTS

L.R.M. is supported by a molecular pathogenesis training grant. J.D.N. is supported in part by NIH Grant AI056070-01A2. J. M. F. is partially supported by DOD Grant DAMD17-03-1-0127.

REFERENCES

Afaq F, Abidi P, Matin R, Rahman Q (1998) Cytotoxicity, pro-oxidant effects and antioxidant depletion in rat lung alveolar macrophages exposed to ultrafine titanium dioxide. *J Appl Toxicol* 18:307–12

Baroli B, Ennas MG, Loffredo F, Isola M, Pinna R, López-Quintela MA (2007) Penetration of metallic nanoparticles in human full-thickness skin. *J Invest Dermatol* 127:1701–12

Chang E, Thekkek N, Yu WW, Colvin VL, Drezek R (2006) Evaluation of quantum dot cytotoxicity based on intracellular uptake. *Small* 12:1412–7

Daum RS (2007) Skin and soft-tissue infections caused by methicillin-resistant *Staphylococcus aureus*. *N Engl J Med* 357:380–90

Friedman AJ, Han G, Navati MS, Chacko M, Gunther L, Alfieri A *et al.* (2008) Sustained release nitric oxide releasing nanoparticles: characterization of a novel delivery platform based on nitrite containing hydrogel/glass composites. *Nitric Oxide* 19:12–20

Gamer AO, Leibold E, van Ravenzwaay B (2006) The in vitro absorption of microfine zinc oxide and titanium dioxide through porcine skin. *Toxicol In Vitro* 20:301–7

Ghaffari A, Miller CC, McMullin B, Ghahary A (2006) Potential application of gaseous nitric oxide as a topical antimicrobial agent. *Nitric Oxide* 14:21–9

Hiramatsu K, Hanaki H, Ino T, Yabuta K, Oguri T, Tenover FC (1997) Methicillin-resistant *Staphylococcus aureus* clinical strain with reduced vancomycin susceptibility. *J Antimicrob Chemother* 40:135–6

Hohr D, Steinfartz Y, Schins RP, Knaapen AM, Martra G, Fubini B *et al.* (2002) The surface area rather than the surface coating determines the acute inflammatory response after instillation of fine and ultrafine TiO2 in the rat. *Int J Hyg Environ Health* 205:239–44

Honing ML, Morrison PJ, Banga JD, Stroes ES, Rabelink TJ (1998) Nitric oxide availability in diabetes mellitus. *Diabetes Metab Rev* 14:241–9

Mowbray M, McLintock S, Weerakoon R, Lomatschinsky N, Jones S, Rossi AG *et al.* (2009) Enzyme-independent NO stores in human skin: quantification and influence of UV radiation. *J Invest Dermatol* 129:834–42

Nel A, Xia T, Mädler L, Li N (2006) Toxic potential of materials at the nanolevel. *Science* 311:622–7

Qi L, Xu Z, Jiang X, Hu C, Zou X (2004) Preparation and antibacterial activity of chitosan nanoparticles. *Carbohydr Res* 339:2693–700

Rabea EI, Badawy ME, Stevens CV, Smagghe G, Steurbaut W (2003) Chitosan as antimicrobial agent: applications and mode of action. *Biomacromolecules* 4:1457–65

Schaffer MR, Tantry U, Gross S, Wasserkrug H, Barbul A (1996) Nitric oxide regulates wound healing. *J Surg Res* 63:237–40

Service RF (2003) Nanomaterials show signs of toxicity. *Science* 300:243

Soneja A, Drews M, Malinski T (2005) Role of nitric oxide, nitroxidative and oxidative stress in wound healing. *Pharmacol Rep* 57:108–19

Zhang X, Broderick M (2000) Amperometric detection of nitric oxide. *Mod Aspects Immunobiol* 1:160–5